Chapter 4: Control Fundamentals of Small / Miniature Helicopters - A Survey[1]

Miniature helicopters are increasingly used in military and civilian applications, mainly due to their ability to hover, fly in very low altitudes and within confined spaces. However, due to model nonlinearities and inherent instabilities, low-level controller design for autonomous flights is a challenge. This Chapter presents an overview of major accomplishments in the area of unmanned helicopter control by several research groups, and focuses on techniques used for low-level control. It then describes a general model suitable for small or miniature helicopter non-aggressive flights and compares three different controllers, a PID, a Linear Quadratic Regulator (LQR) and an $\boldsymbol{H}_\infty$ controller in terms of their practical implementation to achieve autonomous, self-governing flights.

4.1 Introduction

The specific type of unmanned helicopter that is considered in this Chapter is the 'miniature version' of a conventional helicopter with a main rotor and a tail rotor as shown in Figure 4.1. This configuration offers many advantages, but at the same time, it imposes challenges on the design of low-level controllers.

Self-governing flights require generation of low-level signals sent to actuators as well as decision making related to guidance, navigation, path planning, motion planning, mission planning, communications, fault tolerance and emergency landing. When focusing only on sensors and actuators, a thorough understanding of helicopter control issues is needed before designing a controller.

Most control design techniques require at least availability of a system model describing plant dynamics, with higher levels of model details and

---

[1] Written by M. Castillo-Effen, C. Castillo, W. Moreno, K. P. Valavanis. This work has been supported partially by two Research Grants, ARO W911NF-06-1-0069 and SPAWAR N00039-06-C-0062.

Kimon P. Valavanis (ed.), Advances in Unmanned Aerial Vehicles, 73–118.

complexity implying a better approximation. Highly complex models are not practical for most advanced control design methods. For example, controllers designed assuming linear time-invariant models are usually of high order, giving rise to issues related to on-board processing requirements. Model reduction techniques are used to overcome such problems [42] [13]. Concentrating in non-aggressive flights, it is sufficient to evaluate controller design under forward flight and hovering [45].

Fig. 4.1. Small helicopter with a custom-made controller and pan-tilt camera.

Helicopter models are derived from first principles where most parameters have a specific interpretation, or using a 'black box' model where parameters do not have a physical meaning, or using 'hybrid models' that combine the previous two. Regardless, experimental data are required to tune model parameters via system identification techniques.

Models derived from the system's physics, like momentum and blade element theory, provide detailed information related to the physics and plant behavior [44] [45]; when combined, they offer a good balance between complexity and accuracy. The momentum method helps assessing thrust, forces and moments required to keep a helicopter airborne. The blade element method helps computing moments and forces by observing the rotor blades from the aerodynamic perspective. However, derivation of simple and accurate models for model-based control design requires careful judgment.

There is considerable published research in modeling and identification of miniature rotorcraft. In [36], a standard rotorcraft system identification tool called ***C**omprehensive **I**dentification from **Fre**quency **R**esponses* (CIFER) [61] was applied to the Yamaha R-50 and X-Cell 60 miniature helicopters. Scaling rules applied for predicting flying qualities of model helicopters based on known parameters of full-size helicopters were initially studied in [35] and extended in [27] by integrating under the same framework first principles and system identification techniques to a Yamaha R-50 helicopter. This approach was named ***Mo**deling for Flight **S**imulation and **C**ontrol **A**nalysis* (MOSCA). An accurate model of the smaller X-Cell helicopter with significantly different dynamics covering a broad spectrum of its flight envelope was proposed in [14].

The most basic modeling technique requires derivation of equations of motion of the fuselage, assuming that it is a rigid body, following the simple Newton-Euler equations [24] [36] using the concise wrench notation and quaternion algebra [19], or the energy oriented approaches such as the Lagrange formulation [4].

The next Section summarizes efforts in control of miniature rotorcraft, followed by introduction of concepts and specifications before actual controller design to achieve autonomous stable flight. This is followed by modeling fundamentals and an overview of control design techniques suitable for small rotorcraft.

4.2 Contributors to Miniature Helicopter Control

A sample list of major accomplishments on small / miniature helicopter control and research groups that have had an impact on autonomous flight are presented below. The list is neither comprehensive nor the most recent one as the number of groups worldwide conducting research in this area keeps on increasing.

The IARC/AUVSI Competition

The **I**nternational **A**erial **R**obotics **C**ompetition (IARC) has been organized by the **A**ssociation for **U**nmanned **V**ehicle **S**ystems **I**nternational (AUVSI) since 1991. Four missions have been proposed with increasing level of difficulty and realism, being autonomy the main mission tasks requirement.

In its current version, the fourth mission, introduced in 2001, involves several behaviors that must be completed in four qualification levels: i) *L1:* Autonomous flight over a distance of 3 km, waypoint following, hov-

ering over the final waypoint; ii) *L2:* Identifying a target building and open portals autonomously; iii) *L3:* Entering the target structure and relaying reconnaissance information from within; iv) *L4:* While previous levels can be completed in stages, level 4 requires execution of the three previous level behaviors in less than 15 minutes.

No team has completed successfully the fourth mission. According to [18], the mission is 'beyond the capability of any system in existence today, including those of the super-power's military machines'.

The Sugeno Laboratory

Sugeno's research towards achieving autonomous flight control of miniature helicopters dates back to 1988 [41]. Most difficulties associated with autonomous flight were identified and solved to some extent by designing, testing and implementing Fuzzy Logic controllers.

The Carnegie Mellon University Robotics Institute

The CMU Robotics Institute group has reported results on autonomous flight control of helicopters since the early 1990's [3]. The CMU group was the first one that implemented vision-based techniques for navigation, in addition to other traditional sensors commonly used for the same purpose. Besides major accomplishments found in [36] and references therein, recent research in robust control for full-envelope flight control is reported in [26].

Draper Laboratories / MIT

The UAV designed and built at Draper Laboratories, called the ***D****raper* ***S****mall* ***A****utonomous* ***A****erial* ***V****ehicle* (DSAAV), was the only entry in the 1996 AUVSI competition that achieved fully autonomous flight [20].

In 2000, a new approach to UAV aggressive maneuvering using hybrid control techniques was introduced [32]. The main idea was based on incorporating a 'maneuver automaton' that selected optimally different control laws according to the motion primitive that needed be executed. This maneuver automaton concept was developed further and tested in simulation within the framework of the **S**oftware **E**nabled **C**ontrol (SEC) program [46]. An original avionics system and its application to a miniature acrobatic helicopter are also presented in [15] and [58].

The BEAR Project at UC Berkeley

The *aerobo*t research team at UC Berkeley has consistently contributed to

the field of VTOL type UAVs since 1996 [54]. Recent research deals with control of multiple UAVs [53] and the incorporation of obstacle avoidance strategies for navigation in urban environments [51].

The AVATAR Project at USC

Research at the University of Southern California started in 1991 with the first version of an **A**utonomous **F**lying **V**ehicle (AFV), winning the IARC competition in 1994 with the first generation of ***A****utonomous* ***V****ehicle* ***A****erial* ***T****racking* ***a****nd* ***R****etrieval* (AVATAR) helicopters [39]. The AVATAR software and control architecture is further explained in [48] along with other research efforts in autonomous landing and vision-based state estimation. The AVATAR main feature is its hierarchical behavior-based control architecture with all behaviors acting in parallel at different levels. An autonomous landing approach on a moving target and visual servoing in urban areas are the topics discussed in [34] and [50]. Behavior-based architectures for helicopter control have also been reported in [39] [11].

The SEC Program

The Software Enabled Control (SEC) program started in late fiscal year 1999 under Defense Advanced Research Projects Agency (DARPA) funding and sponsorship. Its goal, among other issues, is the search for solutions that would lead to greater levels of autonomy in man-made systems. Realization of complex controls for such systems involves major computational complexity concerns and requires computationally efficient techniques that can be implemented in real-time. Thus, computing plays a prominent role when dealing with such man-made systems and complex controls.

The main focus of the SEC program was to advance control technologies that improve UAV performance, reliability and autonomy. One of the main results was derivation and implementation of an ***O****pen* ***C****ontrol* ***P****latform* (OCP), which enables development and deployment of control functions in terms of objects. In this way, 'object-oriented' control components are distributed across embedded platforms and enable coordination and cooperation among UAVs [46].

Further, a component based design environment called *Ptolemy* was developed, integrated with OCP, to allow for model based control design of heterogeneous systems taking into account the hybrid nature of most technical systems, as well as different models of computation.

Major contributions of the SEC program in the field of low-level VTOL vehicle control are in deriving several Model Predictive Control

(MPC) strategies and the so called *mode transition controller* that blends different linear controllers according to the corresponding appropriate flight mode. To this date, the SEC program has been the most comprehensive effort involving major companies and Universities across the US.

The Georgia Institute of Technology Program

The Georgia Institute of Technology research group is arguably the one group that has contributed the most to the UAV field, not only winning most IARC competitions, but also playing the crucial role in developing and implementing under the DARPA SEC program. Among the main contributions to the unmanned helicopter community the following stand out: i) A prototype implementation of OCP in the form of a fully rigged autonomous helicopter incorporating a fault detection and identification module to compensate for collective actuator failures; ii) A control design methodology for accommodating different flight modes and limit avoidance through mode transition controllers; iii) A helicopter testbed called GTMax, which includes a simulation model of a Yamaha R-Max helicopter with sensors, a ground control station and all baseline on-board routines. The first two components run on Windows platforms and the on-board routines run under QNX.

4.3 Challenges and Specifications

Before any control design takes place, it is essential to define a set of specifications that relate to the mission type and tasks an unmanned helicopter is required to fulfill, which in turn define maneuvers, agility, tracking accuracy and optimality criteria that need be satisfied. Design constraints may depend on physical limitations imposed by the flight mechanics and instrumentation. Availability of information regarding types of disturbances the helicopter will be exposed to, model accuracy and parameter uncertainty are also crucial in defining robustness measures. A limiting factor is the on-board computing capability that will determine the allowable level of software complexity of the control system to be finally implemented.

In manned aerial vehicles, control systems perform different levels of augmentation, while the pilot assesses the ease and precision with which tasks are performed; these are the so called ‘handling qualities’ or ‘flying qualities’ [44]. In unmanned rotorcraft, handling qualities involve artifacts that need be considered as these artifacts will operate at different levels of

autonomy [17]. A valid set of goals and identification of critical missions and payloads has been defined in [64].

Regardless, the complete design cycle of control systems for autonomous unmanned helicopters is subject to severe challenges [57] with the most important listed below:

- Understanding helicopter traits and flight dynamics is a difficult task that requires, almost unavoidably, the use of flight simulators and learning how to pilot small model helicopters in order to acquire an understanding of the process.
- Most system identification techniques cannot be applied directly; hence a well trained pilot is needed to excite the most dominant rotorcraft modes. That is, perform maneuvers that are almost acrobatic while preventing the rotorcraft from crashing
- Data collection for system identification procedures is not a straight forward task, since experiments are limited by fuel autonomy constraints.
- Due to inherent instabilities, it is practically impossible to perform open-loop tests, the exception being hinged test-stands to perform preliminary tests.
- The configuration of the rotors forces a helicopter to act as a gyroscope creating high degrees of coupling between dynamic modes. Modes cannot be easily isolated for analysis usually performed on fixed-wing aircraft, where heave, longitudinal and lateral dynamics have very distinct features.
- Helicopters can perform several types of flights like hovering, flying forward, flying sideward, hovering turn, etc. Flight dynamics are different in each flight mode, so it is very unlikely that a single controller will handle all flight modes.
- Rotors are subject to highly nonlinear quasi-chaotic dynamics due to their turbulent interaction with air and wind gusts. Blades are flexible causing the system to have non-negligible high frequency dynamic components. This is a significant hurdle for deriving a high fidelity lumped model appropriate for control design. Models for high-fidelity simulation are easier to realize through application of computational fluid dynamics (CFD) techniques, albeit not applicable to control design methods.
- Vibration and noise affect main avionic instruments like inertial measurement units, compasses, GPS, etc. This problem may be alleviated, but not completely solved by finding appropriate locations for different instruments, shielding, and applying mechanical damping measures like shock absorbing joints. More recent helicopter designs based on

using electric motors offer improved vibration behavior. However, they usually offer less flight endurance than their combustion engine based counterparts.

- Payload limitations may be the main obstacles in miniature helicopters preventing the use of higher quality instrumentation, vision systems or computing platforms. This factor is tightly coupled to fuel autonomy limitations. The more the payload, the less time the helicopter is able to maintain autonomous flight.

4.4 Modeling and Simulation

This Section begins with a brief introduction to how a helicopter functions, followed by derivation of a model that will be used for simulation and controller design.

4.4.1 Basic Helicopter Function

A helicopter may be studied as a vehicle with six Degrees of Freedom (DOF) that is subject to non-holonomic constraints. It changes its position along three coordinate axes, longitudinal *X*, lateral *Y* and vertical *Z*; its attitude is described by three angles, pitch (θ), roll (ϕ), and yaw (ψ) as shown in Figure 4.2. The configuration space is $SE(3) = R^3 \times SO(3)$. For motion planning purposes, the helicopter configuration space may be reduced to $R^3 \times S^1$ that corresponds to changing the position and heading, since the pitch and roll cannot be chosen arbitrarily.

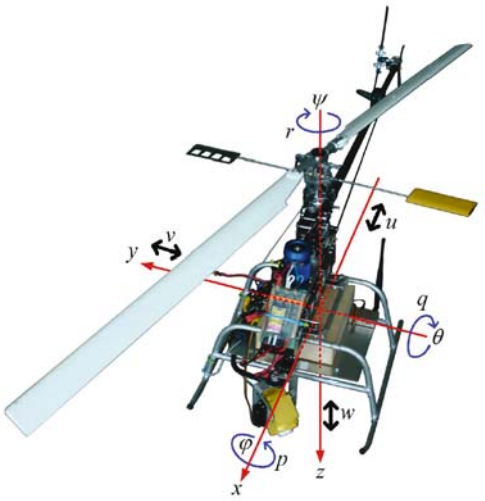

Fig. 4.2. Helicopter and its six degrees of freedom.

Components that produce moments and forces are the helicopter main rotor, the tail rotor, the vertical fin and the horizontal stabilizer. The main rotor blades can change their pitch simultaneously creating different levels of lift. Under manual control mode the pilot may command the pitch of the blades by the *collective* control (u_{col}), used to control heave motion. The main rotor is affected by the *cyclic* control that varies the pitch of the blades cyclically creating different horizontal propulsive forces at different angles. This in turn causes the helicopter to move in the lateral and longitudinal directions. For this reason, cyclic control is usually decomposed into lateral and longitudinal components, u_{lat} and u_{lon}, respectively. Given the rate gyro stabilization mechanism, the pitch of the rear rotor is used to counteract the moment created by the main rotor that can make the helicopter spin. However, the pitch of the rear rotor can also be commanded around the stabilization point allowing the helicopter to change its heading. In real size helicopters this control is accessible through pedals, similar to the rudder in fixed-wing aircraft, thus the name *pedal* control, u_{ped}. The speed of the rotors is usually kept constant through a governor stabilization mechanism within the throttle. When not constant, it creates variable amounts of vertical thrust with a similar effect as the collective control within certain limits.

A component that helps stabilizing longitudinal and lateral dynamics improving ability to fly a model helicopter is the *flybar*. The Bell-Hiller stabilizer bar provides mechanical rate feedback (damping), but it also increases the dynamic complexity of the main rotor and adds aerodynamic

drag. It has been shown that this may be safely eliminated improving closed-loop performance under computer control as well as energy savings, which results in an increase of payload capacity or flight endurance as shown in [22].

4.4.2 Modeling, System Dynamics, System Identification

Considering only the fuselage and the rotors as sources of moments and forces it is possible to derive low-fidelity models used for basic assessment of helicopter handling qualities, but not for simulation or control design. Higher fidelity models require additional state variables that consider model dynamics in higher frequency regions, as well as dynamic features of the rotor such as flapping and coupling between body and main rotor. In most cases, actuators add up additional lags that need be taken into account as first or second order elements.

A key component of a helicopter model is transformation between reference frames. Rigid body equations are derived with respect to the body frame of reference that is fixed on the helicopter. However, to simulate the helicopter in the inertial reference frame, a transformation is needed. If the helicopter attitude is parameterized in terms of Euler angles, the resulting transformations may be given as rotation matrices that are functions of roll, pitch and yaw. Using s, c and t as abbreviations for *sin(.)*, *cos(.)* and *tan(.)*, the respective transformations with variables in the inertial frame on the left hand side and variables in the body frame on the right hand side are:

$$\begin{bmatrix} v_x \\ v_y \\ v_z \end{bmatrix} = \begin{bmatrix} c\theta c\psi & s\phi s\theta c\psi - c\phi s\psi & c\phi s\theta c\psi + s\phi s\psi \\ c\theta s\psi & s\phi s\theta s\psi - c\phi c\psi & c\phi s\theta s\psi - s\phi c\psi \\ -s\theta & s\phi c\theta & c\phi c\theta \end{bmatrix} \begin{bmatrix} u \\ v \\ w \end{bmatrix} \quad (4.1)$$

$$\begin{bmatrix} \dot{\phi} \\ \dot{\theta} \\ \dot{\psi} \end{bmatrix} = \begin{bmatrix} 1 & \sin(\phi)\tan(\theta) & \cos(\phi)\tan(\theta) \\ 0 & \cos(\phi) & -\sin(\theta) \\ 0 & \sin(\phi)\sec(\theta) & \cos(\phi)\sec(\theta) \end{bmatrix} \begin{bmatrix} p \\ q \\ r \end{bmatrix} \quad (4.2)$$

For system identification and control design purposes, the helicopter nonlinear model may be linearized for specific flight regimes [27] [36] [52]. Parameters are extracted such that the model may be written in the state-space form:

$$\dot{\mathbf{x}} = \mathbf{A}\mathbf{x} + \mathbf{B}\mathbf{u} \tag{4.3}$$

with the state vector $\mathbf{x}$ and the control $\mathbf{u}$ given by:

$$\mathbf{x} = \begin{bmatrix} u & v & p & q & \phi & \theta & a & b & w & r & r_{fb} \end{bmatrix}^T \tag{4.4}$$

$$\mathbf{u} = \begin{bmatrix} \delta_{lat} & \delta_{lon} & \delta_{ped} & \delta_{col} \end{bmatrix} \tag{4.5}$$

The state vector includes 11 linear velocity variables[2]: linear velocities in x, y, and z directions, u, v and w, respectively; attitude variables: roll ϕ, and pitch θ; angular rates for roll, pitch and yaw: p, q, and r, respectively; rotor longitudinal and lateral flapping: a and b, respectively; yaw rate gyro feedback r_{fb}.

The control vector is composed from deviations from trim conditions of the four control variables cyclic (δ_{lat}, δ_{lon}), collective (δ_{col}), pedal (δ_{ped}).

The specific state matrices ($\mathbf{A}$, $\mathbf{B}$) for different flying conditions and different types of helicopters, determined through system identification procedures performed before the control system design, have been obtained and tabulated in [52] and [36]. In this Chapter, the parameters obtained for the linearized model of a Yamaha R-50 in hovering flight [36] will be used for assessing application of commonly used techniques for small helicopter control analysis and design. Since parameters are associated with linear models, it is expected that they change according to the current flight mode. The specific parameter values used in [36] are also shown below:

[2] A more basic version of the helicopter model may include only eight state variables, neglecting the last three flapping variables and the yaw rate gyro feedback [51].

$$\mathbf{A} = \begin{bmatrix}
-0.0505 & 0 & 0 & 0 & 0 & -32.2 & -32.2 & 0 & 0 & 0 & 0 & 0 & 0 \\
0 & -0.154 & 0 & 0 & 32.2 & 0 & 0 & 32.2 & 0 & 0 & 0 & 0 & 0 \\
-0.144 & 0.143 & 0 & 0 & 0 & 0 & 0 & 166 & 0 & 0 & 0 & 0 & 0 \\
-0.0561 & -0.0585 & 0 & 0 & 0 & 0 & 82.6 & 0 & 0 & 0 & 0 & 0 & 0 \\
0 & 0 & 1 & 0 & 0 & 0 & 0 & 0 & 0 & 0 & 0 & 0 & 0 \\
0 & 0 & 0 & 1 & 0 & 0 & 0 & 0 & 0 & 0 & 0 & 0 & 0 \\
0 & 0 & 0 & -1 & 0 & 0 & -21.74 & -4.109 & 0 & 0 & 0 & 14 & 0 \\
0 & 0 & -1 & 0 & 0 & 0 & 8 & -21.74 & 0 & 0 & 0 & 0 & 15.43 \\
0 & 0 & 0 & 0 & 0 & 0 & -9.75 & -131 & -0.614 & 0.93 & 0 & 0 & 0 \\
0 & 0.0301 & -3.53 & 0 & 0 & 0 & 0 & 0 & 0.0857 & -4.13 & -33.1 & 0 & 0 \\
0 & 0 & 0 & 0 & 0 & 0 & 0 & 0 & 0 & 2.16 & -8.26 & 0 & 0 \\
0 & 0 & 0 & -1 & 0 & 0 & 0 & 0 & 0 & 0 & 0 & -2.924 & 0 \\
0 & 0 & -1 & 0 & 0 & 0 & 0 & 0 & 0 & 0 & 0 & 0 & -2.924
\end{bmatrix}$$

$$\mathbf{B} = \begin{bmatrix}
0 & 0 & 0 & 0 \\
0 & 0 & 0 & 0 \\
0 & 0 & 0 & 0 \\
0 & 0 & 0 & 0 \\
0 & 0 & 0 & 0 \\
0 & 0 & 0 & 0 \\
0.6804 & -2.174 & 0 & 0 \\
3.043 & 0.3 & 0 & 0 \\
0 & 0 & 0 & -45.8 \\
0 & 0 & 33.1 & -3.33 \\
0 & 0 & 0 & 0 \\
0 & -0.7573 & 0 & 0 \\
0.7982 & 0 & 0 & 0
\end{bmatrix}$$

Given the availability of experimental input - output data and a model as the one in (4.3), there are readily available numerical implementations of Prediction Error Identification Methods (PEM) that allow for optimally determining unknown parameters [29] [30]. Following approaches that resemble Maximum Likelihood Estimation (MLE), PEM methods find estimated parameters by seeking minimization of a function which is a norm of the prediction error sequence, according to:

$$\hat{\theta}_N = \underset{\theta \in D_M}{\operatorname{argmin}} \frac{1}{N} \sum_{t=1}^{N} \ell(\varepsilon_F(t,\theta)) \tag{4.6}$$

The prediction error sequence is a function of the data, the parameters of the assumed model and a stable linear filter $L(q)$:

$$\varepsilon_F(t,\theta) = L(q)\left[y(t) - \hat{y}(t \mid \theta_*)\right] \tag{4.7}$$

Knowing the parameters for a specific flight regime, the main modes that define the key dynamics of the helicopter may be obtained via eigenvalues analysis and exciting the system with the corresponding eigenvectors. Given (4.3), there exist seven basic modes under hovering shown in Table 4.1.

Mode	Natural Frequency (rad/sec)	Damping	Time Constant (seconds)
1	0.32	-0.96	3.27
2	0.41	0.98	2.50
3	0.61	1.00	1.64
4	8.36	0.20	0.59
5	11.86	0.22	0.38
6	10.28	0.60	0.16
7	20.86	0.97	0.05

Table 4.1. Modes in hovering flight.

Mode 1 is an unstable slow phugoid mode that affects mainly the lateral and longitudinal linear velocities. Mode 2 is a barely under damped stable phugoid mode involving the horizontal and vertical linear velocities. Mode 3 is a damped mode affecting the heave velocity. Mode 4 is an under damped mode involving roll, pitch and yaw angular rates, as well as the heave velocity. This mode shows clearly the gyroscopic coupling between rotational speeds. It illustrates the fact that attitude dynamics is faster than translational dynamics. Mode 5 is an under damped mode affecting the pitch angular rate and the heave velocity. Mode 6 is a relatively fast under damped mode showing coupling between yaw and heave velocity. Mode 7 is a fast critically damped mode that shows strong coupling between fast changes in pitch and heave velocity.

This modal analysis illustrates the degree of coupling among different state variables at specific frequencies and helps obtaining a better understanding of plant dynamics. It may be used to verify qualitatively correctness of system identification procedures.

Figure 4.3 shows the plot of singular values against frequencies for the used linearized model and obtained modes. The plot provides a graphical tool for obtaining a measure of the magnitude of the gain of a multivariable system.

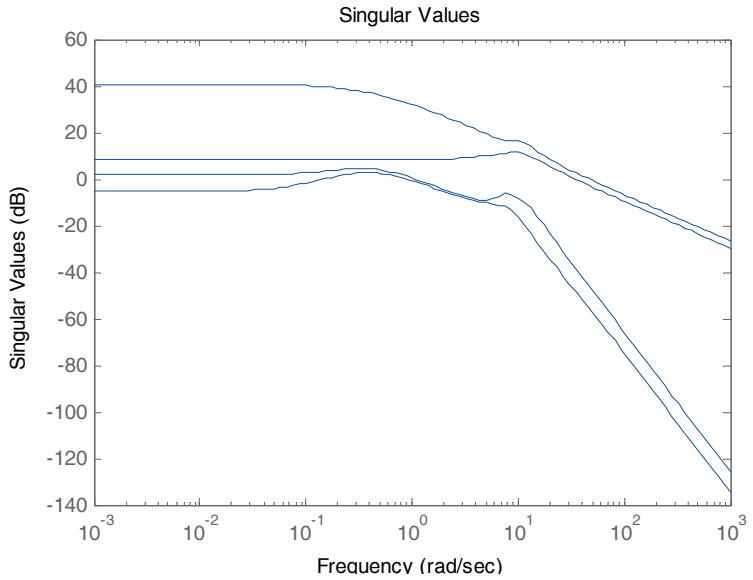

Fig. 4.3. Singular values of Yamaha R-50 in hovering mode.

The largest singular value starts declining at a corner frequency of 0.4rad/sec at -20dB/Dec. The smallest singular value decays rapidly after 10rad/sec at -60dB/Dec. A resonant peak appears to take place around 10rad/sec. The frequency response shows that in general, most relevant features are found between 0.1rad/sec and 100rad/sec.

One attribute of helicopter dynamics with important implications for control design is the non-minimum phase characteristic. This means that when linearized, the model has transmission zeros in the right half plane. This fact has been proven in [25], used in [54], and confirmed in [12] and [37]. Non-minimum phase systems present and additional challenge for application of certain control methods such as in Linear Quadratic Control / Loop Transfer Recovery (LQR/LTR) or for dynamic inversion procedures. It has been shown that under certain assumptions, the system may be analyzed as being minimum-phase as highlighted in [54] by using the term ‘slightly non-minimum phase’.

4.5 Overview of Control Techniques

Controller design for small unmanned helicopters requires addressing and overcoming at least the following characteristics that are specific to these flying machines:

- High degree of coupling among different state vector different variables.
- Nonlinear behavior that makes the linear model valid only for certain regions of the flight envelope.
- Difficulties associated with obtaining accurate models due to issues related to application of standard system identification procedures and methodologies, resulting in models with high parameter uncertainty.
- Open-loop instability.
- Dynamics spanning a wide range of frequencies.
- Very fast dynamics, especially in the case of very small model helicopters.
- Diverse sources of noise and disturbances. The helicopter is subject to effects of rotor wake, wind gusts, and vibrations. To reduce payload the avionics system incorporates lower grade instruments and sensors that increase measurement noise. Light structures imply flexibility, a major source of unmodeled dynamics.

To overcome such difficulties, modern ***C****omputer-****A****ided* ***C****ontrol* ***S****ystem* ***D****esign* (CACSD) technologies offer tools to design controllers that satisfy conditions imposed by different applications. Basic approaches and commonly used techniques for design of helicopter control systems are elaborated next, putting emphasis on simplified techniques with practical relevance.

4.5.1 Low-Level Control Architecture

There exist low-level control structures that may serve as a foundation for new approaches to designing small helicopter controllers, or for application of already well-known methodologies.

Cascaded Control

Based on prior experience in piloted aeronautical vehicles [1], the cascaded control approach [21] [47] considers that the helicopter control system is decomposed into two loops where reference signals for the inner-loop are produced by controllers in the outer-loop as shown in Figure 4.4.

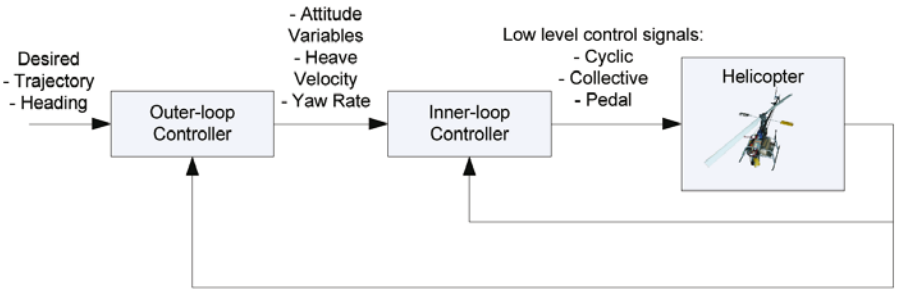

Fig. 4.4. Inner- and outer- loop cascaded control.

The inner-loop stabilizes the helicopter and decouples state variables controlling attitude. Typically, design of the inner-loop aims at achieving high bandwidth and robust stability. The outer-loop is used for guidance, generating velocity commands for the inner-loop. It operates at a slower time scale than the inner-loop.

Further, one of the main tasks of the inner-loop is to provide adequate decoupling such that outer-loop controllers may control each variable independently. Hence, a coupling metric is used to evaluate the degree of success with which the inner-loop controllers achieves decoupling.

Viewed from the behavior-based robotics perspective, the inner-loop may be considered as a set of reactive behaviors that act at the lowest level of a 'subsumption architecture' [7], while the outer-loop includes behaviors with higher levels of competence.

Sensor Fusion in Miniature Helicopters

Sensor fusion is essential for estimating non-measurable state variables and filtering, and also for performing system identification procedures. The main task of the data fusion module is to yield optimal estimates for key state variables using sensor measurements. State estimation techniques are also needed since almost all most small helicopters are equipped with low cost light-weight sensors prone to noisy measurements at different data rates and they are subject to considerable vibration and turbulent gusts. Reference [49] offers an excellent comparative overview of avionic systems and sensor fusion algorithms of some of the early autonomous helicopter projects. However, small helicopters are equipped at a minimum with the following sensors:

- An on-board Inertial Measurement Unit (IMU) with three angular rate gyros, three orthogonal accelerometers and three orthogonal magnetometers to measure the Earth's magnetic field, measuring dynamic and static attitude of the rotorcraft. The challenge is in estimating and eliminating bias drift in IMU measurements. This may be accom-

plished by including biases as states, and by applying a period of pre-flight warm up. Attitude measurements may be obtained at relatively short sampling intervals, 10ms or 100Hz. When the IMU does not include magnetometers, they need be added externally.

- A Global Positioning System (GPS) receiver that supplies position estimates. GPS receivers have several sources of errors such as atmospheric and multi path effects. Four satellites need be in the Line of Sight (LOS) of the receiver – 'GPS lock'. GPS are relatively slow measurement devices and samples can generally obtained at 1Hz, with temporary dropouts when GPS lock is lost. A similar technology called differential GPS may provide very accurate position estimates (2 cm) with the main disadvantage being the need of a base station with a precisely known location and higher cost of the receiver.
- A barometric altimeter that is used to provide altitude information. This measurement may be considered complementary to GPS readings. Measurements are relatively slow (20Hz) and noisy. However, sensor fusion filters can successfully eliminate it. For lower altitudes, in particular for enabling autonomous take-off and landing maneuvers, ultrasound sensors and radar may also provide accurate altitude readings.

The Kalman filter (KF) calculates optimal estimates provided that two main conditions are met: the system is linear and noise is Gaussian [8] [56] [65]. Since helicopter motion equations are evidently nonlinear and sensor noise is not necessarily Gaussian, the extended Kalman filter (EKF) relaxes the linearity condition by applying linearization of the model, implemented in two steps of prediction and update. The EKF computational complexity is not greater than the KF; therefore, it is best to follow the EKF recursive estimation equations.

To derive the EKF equations, it is necessary to know the magnitude and model sensor noise and system noise associated with the helicopter model. The helicopter model may not incorporate the full state vector of (4.4) but only the state variables of the kinematics model. However, the state vector may be augmented with the gyro biases to account for the required assumption of Gaussian noise. The EKF state vector $\mathbf{x}$ usually includes the inertial position x, y, z, the body frame velocities: u, v, w, the attitude quaternion: e_0, e_1, e_2, e_3, and the gyro biases: p_{bias}, q_{bias} and r_{bias}. The system equation based on kinematics has the form:

$$\dot{\mathbf{x}} = f(\mathbf{x}, \mathbf{a}, \omega) + vN(0, Q) \tag{4.8}$$

In (4.8), $\mathbf{a}$ and ω are measured accelerations and angular rates; its discrete-time version yields the state estimate $\hat{\mathbf{x}}$ according to the kinematics model, while the system matrix $\mathbf{F}$ is obtained (before obtaining the Kalman gain) calculating the Jacobian of the function $f(\cdot)$:

$$\mathbf{F} = \left.\frac{\partial f}{\partial \mathbf{x}}\right|_{\mathbf{x}=\hat{\mathbf{x}}} \tag{4.9}$$

Additional sensing information from cameras can be added to the standard instrumentation list shown above. Successful incorporation of vision to the instrumentation system of autonomous helicopters has been documented in [9] and [34].

4.5.2 Control Techniques Applied to Helicopter Flight Regimes

Linear controllers allow for determining exact measures of closed-loop performance, stability and robustness. Nonetheless, these techniques rely on the strong assumption of the plant being linear, which holds true only for a region of the state-space around an operating point. When a nonlinear system traverses different regions of the state space, several linear models may be used to approximate the overall nonlinear dynamics. Thus, several controllers need be designed and 'activated' according to the linear model that approximates best local dynamics. Since the controllers do not necessarily have different structures, only parameters may need to change giving rise to a gain-scheduling scheme. If controllers with different structures are needed, blending techniques may be necessary to achieve smooth transitions between them, as illustrated in Figure 4.5.

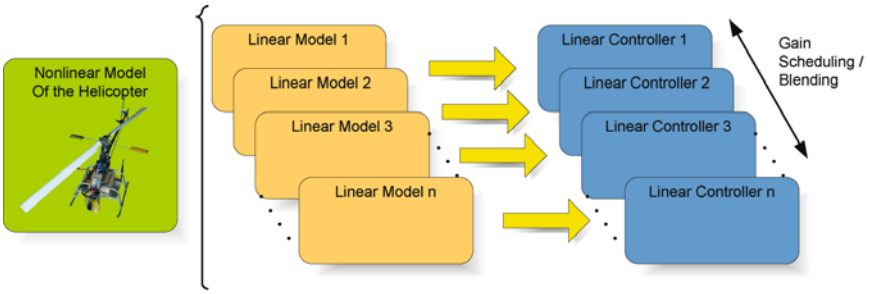

Fig. 4.5. Divide and conquer approach - linear control.

Coupling Analysis

The helicopter as a whole may be considered as a square system with four inputs and outputs as shown in Figure 4.6, with the best input / output pairing shown in Table 4.2.

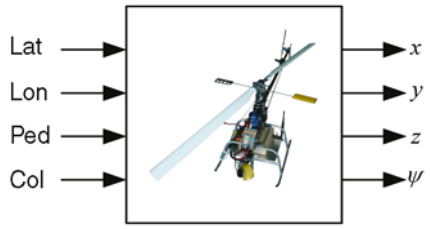

Fig. 4.6. Helicopter viewed as a square system.

Input	Pairing
Lateral Cyclic (u_{lat}), Longitudinal Cyclic (u_{lon})	Position in Horizontal Plane (x, y)
Collective (u_{col})	Altitude (z)
Pedal (u_{ped})	Yaw (ψ)

Table 4.2. Input/output pairing.

However, following decomposition in inner- and outer- loop, internal variables to be paired with inputs are not as unequivocal. The most commonly used input / output pairs for the inner-loop controller are shown in Table 4.3, with each pair often referred to as 'channel', sometimes treated in isolation for tuning purposes.

Input	Pairing 1	Pairing 2
Lateral Cyclic (u_{lat})	Roll (ϕ)	Lateral speed (v)
Longitudinal Cyclic (u_{lon})	Pitch (θ)	Longitudinal speed (u)
Pedal (u_{ped})	Yaw rate (r)	Yaw rate (r)
Collective (u_{col})	Heave velocity (w)	Heave velocity (w)

Table 4.3. Most commonly used input/output pairings.

Two main metrics are considered to quantify the degree of interaction among channels justifying a particular pairing: the relative gain array (RGA), or gain array number, RGAN, and diagonal dominance. The $(i, j)^{\text{th}}$ element of the RGA $\Lambda(\omega)$ [16] [57] is calculated for all relevant frequencies as:

$$\lambda_{ij} = [G(\omega)]_{ij}\left[G^{-1}(\omega)\right]_{ji} \tag{4.10}$$

The RGAN summarizes results obtained from the RGA into one number according to:

$$\text{RGA number} \triangleq \left\|\Lambda(G) - I\right\|_{\text{sum}} \tag{4.11}$$

Here $\left\|A\right\|_{\text{sum}} = \sum_{i,j} |\, a_{ij} \,|$. It penalizes the off-diagonal elements; therefore smaller RGAN implies better decoupling.

For a square system with n inputs and outputs, diagonal dominance is also used to verify decoupling, its elements being computed as a function of frequency according to:

$$\Phi_j(j\omega) = \frac{\sum_{i=1, i\neq j}^{n} |\, z_{ij}(j\omega) \,|}{|\, z_{jj}(j\omega) \,|} \tag{4.12}$$

Values that are smaller than 1 indicate a level of diagonal dominance that allows for decoupling. Values greater than 1 indicate high degree of coupling.

Considering the linear model of the Yamaha R-50 in hovering flight, Figures 4.7 and 4.8 depict the RGAN and diagonal dominance for the two pairings of Table 4.3.

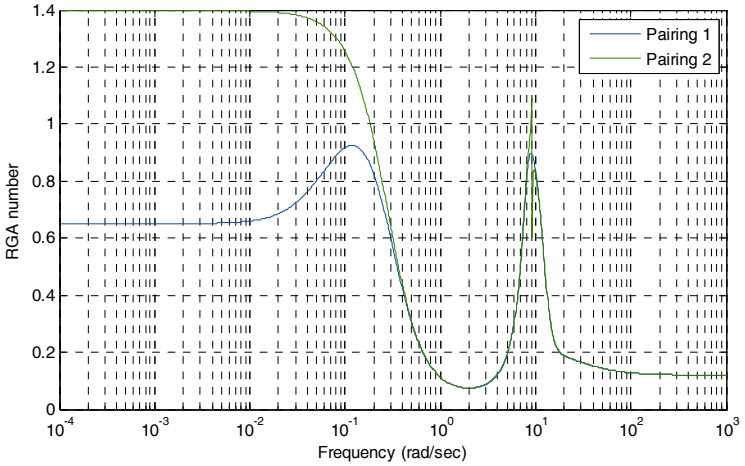

Fig. 4.7. RGAN; Yamaha R-50 model, hover condition.

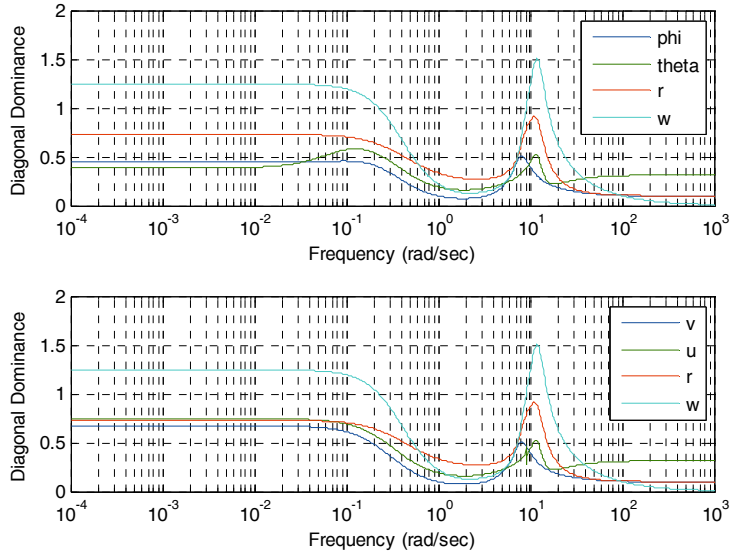

Fig. 4.8. Diagonal dominance; Yamaha R-50 model, hover condition.

In general, it may be concluded that the helicopter behaves strongly as a set of two Two-Input / Two-Output (TITO) system given the coupling between the lateral and longitudinal channels, as well as the coupling between the pedal and collective channels. The latter two may be also approximated by two Single-Input / Single-Output, SISO, channels. The out-

put affected by most of the inputs is the heave velocity. The pedal and collective inputs do not have much influence on the upper TITO system containing the longitudinal and lateral cyclic. From Figures 4.7 and 4.8 it may be concluded that the first pairing represents a slightly better choice since values are smaller.

Robustness Analysis

Robustness analysis helps quantify control system stability and performance under all possible sources of uncertainty and disturbances. UAV deployment does involve factors contributing to unexpected behavior. Therefore, plant modeling but also the uncertainty resulting from the mismatch between a nominal model and the real plant need be considered. Since a 'perfect' physical plant model is unachievable, the helicopter dynamic behavior is described by a set of possible linear time-invariant (LTI) models Π [57]. During flight any perturbed model $G'(s) \in \Pi$ may be valid as in Figure 4.5 where each linear model may be seen as a model incorporating uncertainty. A robust controller must guarantee stability and predefined performance.

Considering SISO systems, phase and gain margins are usually a good measure of 'slack' before reaching instability. Robustness analysis in MIMO systems requires more elaborate development as gain and phase margins of the transfer function matrix elements do not provide sufficient information. The generalized configuration depicted in Figure 4.9 will be studied.

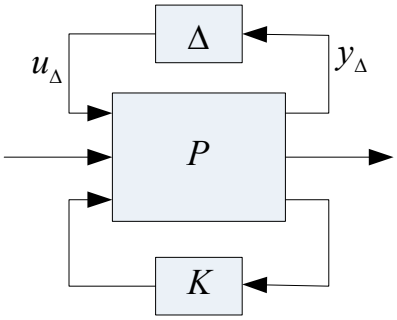

Fig. 4.9. Generalized control configuration.

Blocks P, K and Δ represent the plant, the controller, and source of uncertainties. w models all exogenous inputs to the system. z represents all variables that need be controlled, including performance variables with small desired value. u represents controller inputs and v all sensor meas-

urements. The transfer function from inputs u_Δ, w to output z has to be small in all relevant frequencies and directions. The system of Figure 4.9 is described by [57]:

$$\begin{bmatrix} z \\ v \end{bmatrix} = P(s) \begin{bmatrix} w \\ u \end{bmatrix} = \begin{bmatrix} P_{11}(s) & P_{12}(s) \\ P_{21}(s) & P_{22}(s) \end{bmatrix} \begin{bmatrix} w \\ u \end{bmatrix} \tag{4.13}$$

with $$z = [P_{11} + P_{12}K(I - P_{22}K)^{-1}P_{21}]w = F_l(P,K)w \tag{4.14}$$

The block diagram of Figure 4.10 shows a one degree-of-freedom controller that will be considered to connect robustness with the traditional frequency shaping followed in SISO system design and understand the importance of *sensitivity functions*. Design constraints and closed-loop requirements will be met by 'playing' with the singular values of the open-loop system.

Observing Figure 4.10, relevant multivariable transfer functions may be defined [66] [5] [57]: the loop transfer matrix $L = GK$, the sensitivity function $S = (I + L)^{-1}$ and the complementary sensitivity function $T = L(I + L)^{-1}$ such that $S + T = I$.

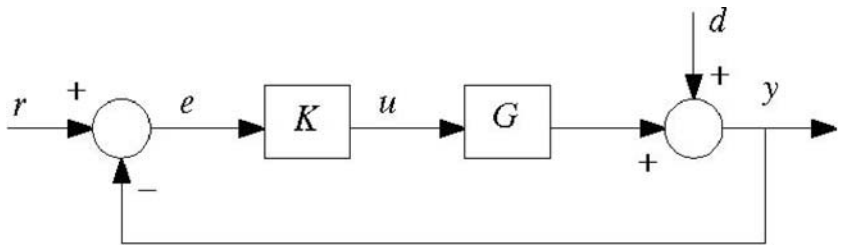

Fig. 4.10. One degree-of-freedom control configuration.

Therefore, the closed-loop response, the control error and control effort may be obtained, respectively, in terms of L, S and T, as follows:

$$y = Tr + Sd \tag{4.15}$$

$$e = S(d - r) \tag{4.16}$$

$$u = KS(r - d) \tag{4.17}$$

The greatest and smallest singular value of the particular transfer function at a particular frequency is utilized to quantify their magnitude. For example, the condition for desentization of y with respect to disturbances in a specific frequency band (where the attenuation factor $W_1 \geq 1$ varies with frequency) can be given by:

$$\bar{\sigma}(S(j\omega)) \leq W_1^{-1}(j\omega) \tag{4.18}$$

For reference tracking, the condition $\bar{\sigma}(T(j\omega)) \approx \underline{\sigma}(T(j\omega)) \approx 1$ should be fulfilled. The control effort can also be reduced by keeping $\bar{\sigma}(KS(j\omega))$ bounded. The same condition helps achieving robust stability when plant uncertainty is modeled as an additive perturbation, that is, $G_p = G + \Delta$. When plant uncertainty is modeled as a multiplicative output perturbation $G_p = (I + \Delta)G$, then $\bar{\sigma}(T(j\omega))$ needs be kept small:

$$\bar{\sigma}(T(j\omega)) \leq W_2^{-1}(j\omega) \tag{4.19}$$

It is easily verified that for low /high frequencies, respectively:

$$\frac{1}{\bar{\sigma}(S(j\omega))} \approx \underline{\sigma}(L(j\omega)) \tag{4.20}$$

$$\bar{\sigma}(T(j\omega)) \approx \bar{\sigma}(L(j\omega)) \tag{4.21}$$

Loop shaping constraints are shown in Figure 4.11.

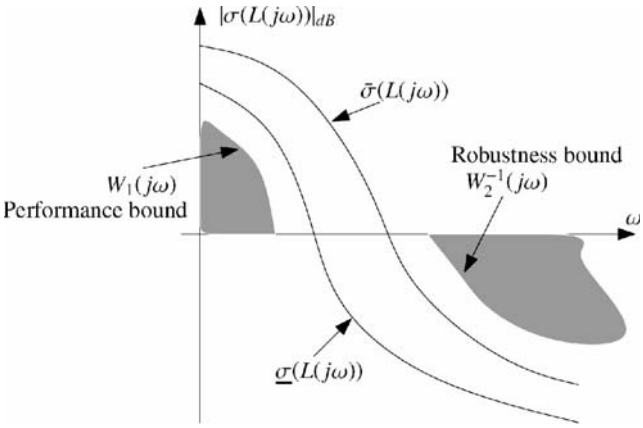

Fig. 4.11. Loop shaping constraints.

As previously mentioned, the Yamaha R-50 parameters obtained via system identification procedures have tolerances, and the parameters presented in Section 4.4.2 represent only dynamics of the nominal model. Further, the state variables of (4.3) are handled in the body-fixed frame, but the actual rotorcraft needs be controlled in the earth-fixed frame. The transformation (4.1) between the two reference frames introduces a nonlinearity that may be accounted for as 'uncertainty factor'. Figure 4.12 shows a similar frequency response as Figure 4.3 with variations that result from uncertainties; this singular value plot includes uncertainties due to variations of pitch and roll of $\pm 20^{\circ}$.

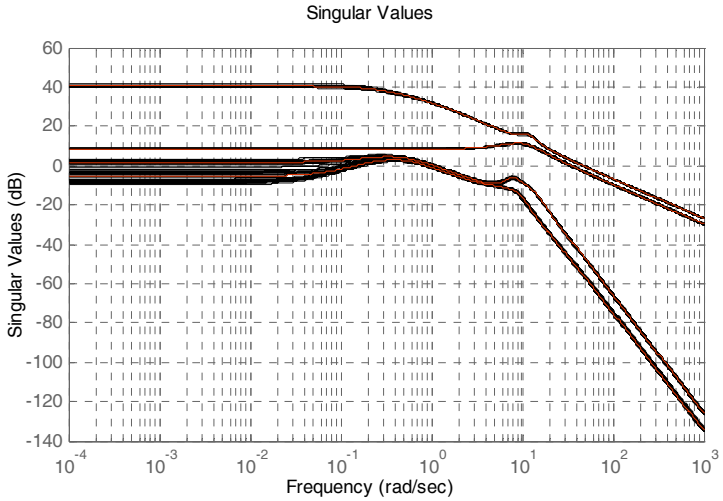

Fig. 4.12 Singular values of Yamaha R-50 considering uncertainties.

PID Controllers

Most initial attempts to achieve autonomous helicopter flight have been based on PID controller design [2] [23] [36]. Most commercial autopilots such as Micropilot's MP2128-Heli [38] or Rotomotion's AFCSV2.5 UAV Helicopter Controller [62] are based on PID controllers.

PID controller parameters may be easily adjusted allowing for on-line tuning when the model is not known. On the other hand when a sort of accurate model is given, classical design or optimization-based tuning strategies may be attempted [10]. The main disadvantage of SISO PID controllers relates to overlooking coupling among controlled variables, limiting bandwidth and agility that could be achieved. However, since standard

PID controllers are of the SISO type, it is assumed implicitly that controlled variables are not strongly coupled. Figure 4.13 shows the helicopter decentralized inner-loop controller structure based on PID controllers.

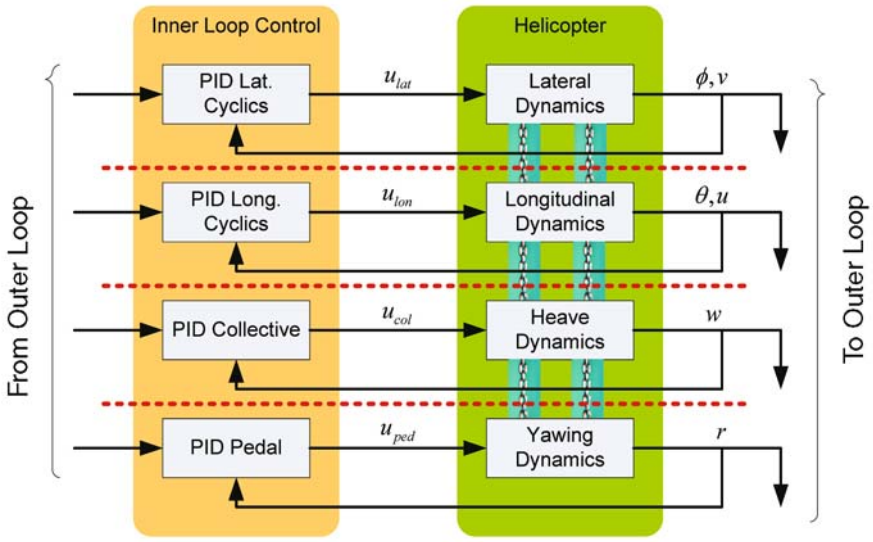

Fig. 4.13. Inner-loop PID controllers.

For the Yamaha R-50 PID controllers are assigned to each channel of the plant. The best flexibility is obtained when using two-degree-of-freedom PID controllers as shown in Figure 4.14 with an anti-windup term at the output preventing saturation.

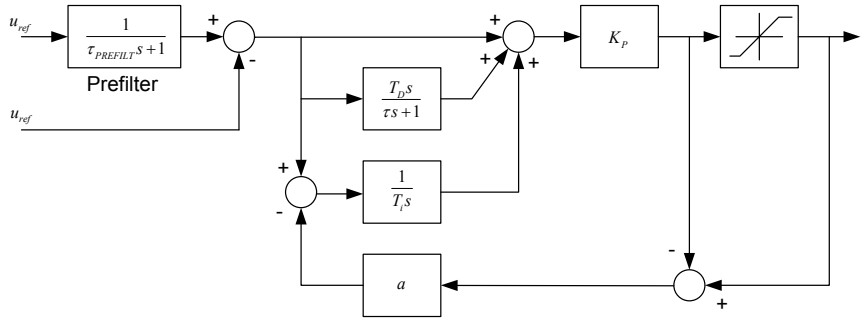

Fig. 4.14. Structure of a 2-DOF PID controller.

The lateral and longitudinal channels controlled by the PID compensators cannot be tuned individually since the diagonal terms of the matrix transfer function present unstable non-minimum phase dynamics. However, iterative tuning of the controllers, starting from rough hand-tuning,

gives very good results as validated through experiments conducted with the controlled plant. PID controllers have been parameterized using the following standard form given by [16]:

$$C_{\text{PID}}(s) = K_p\left(1+\frac{1}{T_i s}+\frac{T_d s}{\tau s+1}\right) \tag{4.22}$$

Parameters for all four Yamaha R-50 PID controllers are listed in Table 4.4.

Channel	K_p	T_i	T_d	τ
Lateral	1.63	0.48	0.096	0.02
Longitudinal	2.17	0.333	0.058	0.017
Pedal	3.74	0.374	0	0
Collective	9.83	0.983	0.120	0.05

Table 4.4. PID parameters for inner-loop controllers.

Figure 4.15 illustrates the behavior of the PID controllers with respect to decoupling using diagonal dominance. The values for the open-loop plant are also included for comparison purposes.

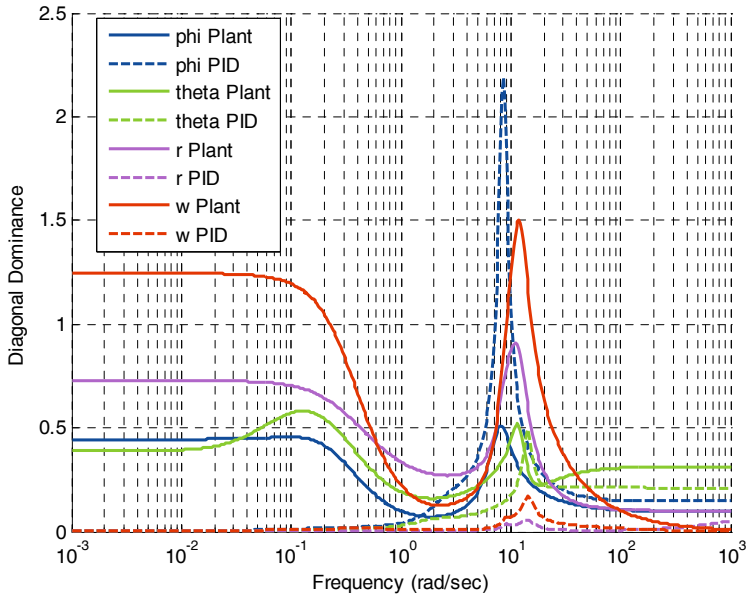

Fig. 4.15. Inner-loop decoupling effect using PID controllers.

The singular values of the open-loop transfer function matrix are shown in Figure 4.16. Singular values of the plant alone are also included to observe the effect of the control on the loop shape.

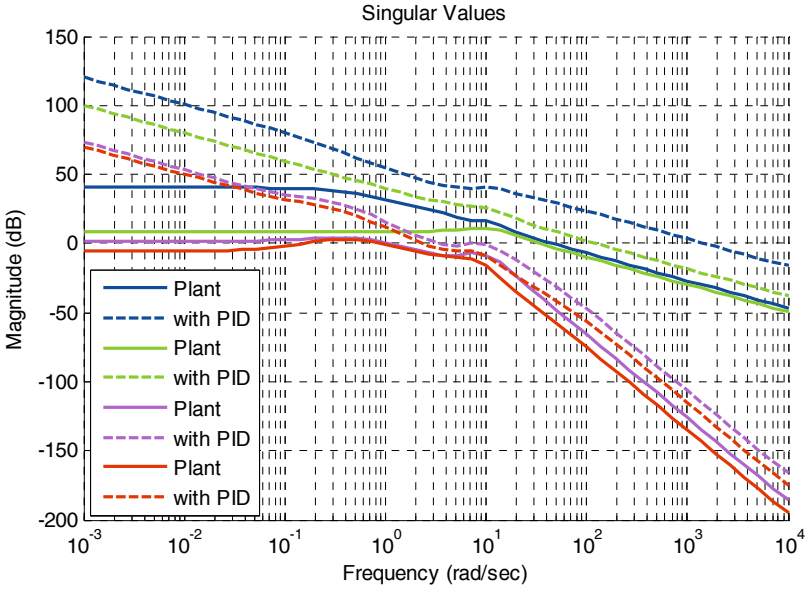

Fig. 4.16. Singular values of the PID control loop.

The singular values show that the integral action provides high gain at lower frequencies, guaranteeing good decoupling and low steady state errors. High gain at lower frequencies contributes to achieving a high level of agility. High gains at high frequencies indicate potential problems with respect to noise sensitivity, especially sensor noise, and high gains at higher frequencies points to potential robustness problems.

Linear Quadratic Control Techniques

When the plant model is considered as a full MIMO system, the first systematic technique to control the helicopter is the linear quadratic regulator (LQR) design methodology [13] [55] [58]. LQR control has been applied successfully to aeronautical control problems [60] mainly due to guaranteed robust asymptotic stability of the closed-loop. However, stability measures are only valid under the assumption of full state noise-free feedback and perfect knowledge of the model. In reality, the helicopter's nonlinearity makes the model valid within a region around a specific operating point used for design. Furthermore, not all state variables can be meas-

ured, therefore, applying a filter-observer as previously discussed may be required. Even in this case, robustness properties do not hold anymore, unless observer dynamics are much faster than rotorcraft dynamics.

In any case, noise presence in measured signals requires studying the problem from the stochastic systems perspective. Under this perspective, the linear quadratic Gaussian (LQG) control methodology (design) requires obtaining the linear quadratic controller and determining an optimal observer. Implementation, design procedures and experimental results of LQG control applied to miniature helicopters have been documented in [6], [40] and [64]. Designs may be obtained using numerical routines included in standard CACSD packages [31].

In detail, LQR is a full-state feedback control where x is the state vector and u is the control effort designed to minimize the quadratic performance measure described by:

$$V = \int_0^T (x'Qx + u'Ru)dt \tag{4.23}$$

The weighting matrices Q and R are design parameters varied to obtain a specified closed-loop dynamic behavior, pole placement, penalizing control accuracy and control effort, respectively. Since (4.23) has Q and R in two bilinear forms, they need be positive semi-definite and positive definite, respectively, $Q = Q^T \geq 0$, $R = R^T > 0$. This minimization problem is translated to the solution of an algebraic Riccati equation given by:

$$A^T X + XA - XBR^{-1}B^T X + Q = 0 \tag{4.24}$$

with a positive semi-definite solution X and control law:

$$u = -K_r x\ ,\ K_r = R^{-1}B^T X \tag{4.25}$$

Design of an optimal observer under the assumption of Gaussian noise leads also to an Algebraic Riccati equation whose solution yields a Kalman filter. The combination of optimal estimator and linear quadratic regulator gives the LQG controller. The two components plus integral action for tracking reference signals are shown in Figure 4.17 applicable to helicopter control.

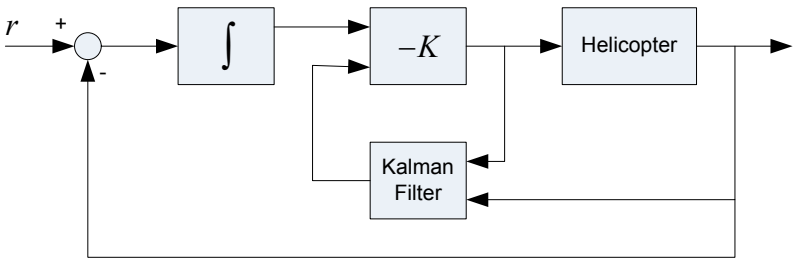

Fig. 4.17. LQG controller as combination of a KF and state feedback [57].

In order to guarantee certain robustness properties, particularly considering the frequency behavior of sensitivity functions over specific frequency ranges, frequency dependent Q and R weight matrices need be considered in (4.23). To achieve this, it is possible to augment the open-loop system with fictitious states and apply the standard LQG design procedure with the help of computerized tools. This method results in gains that are not static but have the form of dynamic compensators. This extension of the LQG methodology is also known as Wiener-Hopf design or H_2 control. In the case of the H_2 controller, the energy of the impulse response of the fictitious plant G is minimized:

$$\| G \|_2 = \sqrt{\frac{1}{2\pi} \int_{-\infty}^{\infty} \mathrm{tr}\left[G(j\omega) G^*(j\omega) \right] d\omega} \tag{4.26}$$

Although H_2 optimal control design is easily accomplished using CACSD tools, considering that the plant is open-loop unstable in some of its flight regimes, one should take into account (in order to avoid unexpected behavior) measures such as the integrated log of sensitivity magnitude [59]:

$$\int_0^{\infty} \ln | \det S(j\omega) | \, d\omega = \pi \sum_{i=1}^{N_p} \mathrm{Re}(p_i) \tag{4.27}$$

Here, $S(j\omega)$ represents the frequency dependent sensitivity function considered in its MIMO form and the summation in the right term is carried over the poles (controller and plant) that lie on the right half plane (RHP).

For the Yamaha R-50, an output feedback LQG controller with integral action has been designed assuming measurement availability of the inner-loop controlled variables. The plant has been augmented with free integrators for high open-loop gain at lower frequencies, achieving good tracking accuracy and mainly good decoupling. An LQR regulator has been designed assuming knowledge of the complete state vector with $Q = 0_{17\times17}$ and $R = \begin{bmatrix}0.5 & 0.02 & 0.025 & 10\end{bmatrix} \times I_{13\times13}$. The Q matrix has four more terms since it includes the states associated with the augmented integrators.

Design of the KF involves selection of weights for process and measurement noise, W and V, respectively, both set to identity matrices for simplicity purposes. The states of the integrators do not need be estimated, hence $W = I_{13\times13}$ and $V = I_{4\times4}$.

The resulting design can be seen as a 2-DOF controller shown in Figure 4.18. The integrators have been isolated from the controller to enable an anti-windup scheme by using limited outputs.

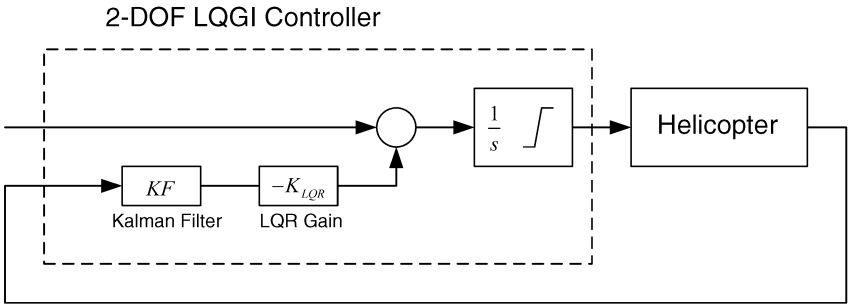

Fig. 4.18. LQG with integrator.

Figure 4.19 presents the resulting diagonal dominance values along with those of the plant.

Singular values of the open-loop system are shown in Figure 4.20 and compared against the plant. In general, the loop presents lower gains at lower frequencies in comparison to the PID design. Much lower gains at higher frequencies show a very good behavior concerning sensor noise. Low noise sensitivity is achieved at the expense of slightly lower bandwidth, thus agility is not as good as in the case of the PID design.

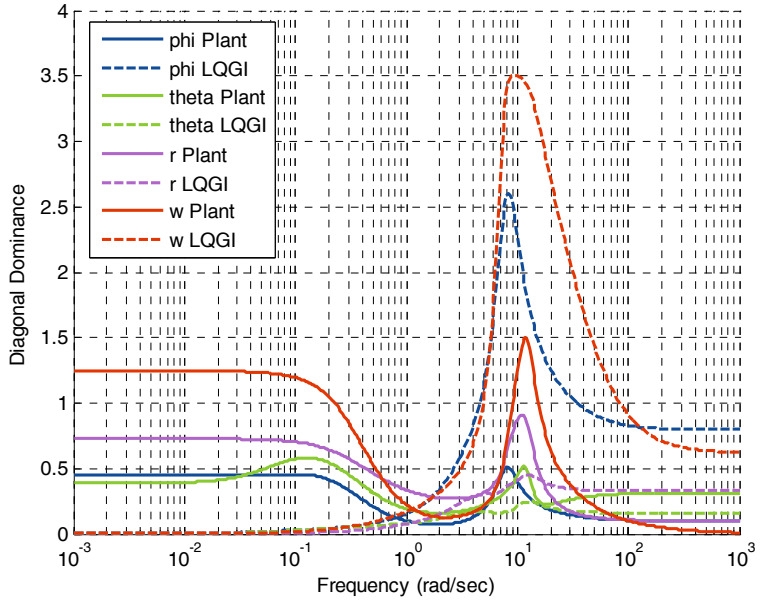

Fig. 4.19. Inner-loop decoupling using LQG control with integration.

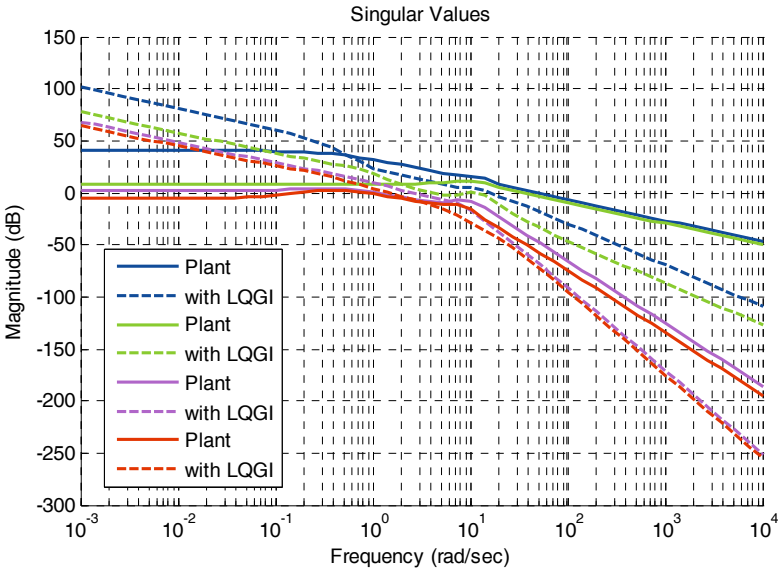

Fig. 4.20. Singular values of the LQGI control loop.

Robust control design

Robust control represents the most widely used and proven design technique for small-scale helicopters allowing for aggressive maneuvers exploiting their agile dynamics. Robust controllers have been reported to perform better than LQG controllers since they address robustness measures directly in the controller synthesis process [6] [26] [28] [40] [54] [64], while seminal work in robust control has been reported in [5] [57] [66] and [67]. Robust control offers several techniques for synthesis of robust MIMO controllers with CACSD tools supporting most of these methods [5] including *MATLAB's* robust control toolbox.

The H_2 and H_∞ optimal control tasks consist of finding controllers that minimize specific norms of $F_l(P,K)$, with:

$$\left\|F\right\|_2 = \sqrt{\frac{1}{2\pi}\int_{-\infty}^{\infty} \mathrm{tr}\left[F(j\omega)F^*(j\omega)\right]d\omega} \tag{4.28}$$

$$\left\|F\right\|_\infty = \sup_{\omega} \bar{\sigma}\left[F(j\omega)\right] \tag{4.29}$$

An H_∞ multivariable robust controller with loop shaping is now designed with the same previously used linearized model as basis for development. The design methodology follows the loop shaping methodology presented in [33] and applied to the Yamaha R-50 [26]. The objective is to design an optimal loop-shaping controller for the inner-loop with the goal of providing robust attitude stabilization and decoupling of the main four channels. The design technique follows three main steps:

- The nominal plant G is augmented with a pre-compensator W_1 and a post-compensator W_2 in order to shape the singular values of the open-loop transfer function. The augmented plant is $G_s = W_2 G W_1$, with W_1 defining the controller behavior at lower frequencies trying to obtain high gain, which in turn yields good tracking behavior and decoupling and disturbance rejection. For these reasons, PI-type frequency shapes are selected. For W_2, the objective is to provide enough damping at higher frequencies guaranteeing robustness. This is accomplished by selecting low pass filters and constant gain terms; as in [26] the following weighting functions are proposed:

$$W_{1,lat} = \frac{1.13s+3.4}{s} \quad W_{1,lon} = \frac{1.63s+6.50}{s} \quad W_{1,ped} = \frac{3.74s+37.4}{s} \quad W_{1,col} = \frac{8.33s+10}{s}$$

$$W_{2,lat}=1 \quad W_{2,lon}=1.14 \quad W_{2,ped}=\frac{2028}{s^2+80s+2500} \quad W_{2,col}=\frac{2795}{s^2+80s+2500}$$

Both, W_1 and W_2 are diagonal matrices, having the terms above in the main diagonal.

- Find an optimal controller K_∞ that minimizes the H_∞ norm of the transfer function from disturbances to errors - γ is between 1 and 3:

$$\min_{K_\infty}\left\|\begin{bmatrix} I \\ K_\infty \end{bmatrix}(I-G_sK_\infty))^{-1}[G_s,I]\right\|_\infty=\gamma=\varepsilon^{-1}$$

using the `ncfsyn` function from the *MATLAB* robust control toolbox, `[K,CL,GAM]=ncfsyn(G,W1,W2)`

- Construct the feedback controller by combining the synthesized K_∞ controller with W_1 and W_2, such that $K=W_1K_\infty W_2$

After execution, the `ncfsyn` function returns a valid K_∞ controller, the closed-loop system, and the margin $\gamma=2.68$ that is within the acceptable interval. Figure 4.21 shows the singular values of three systems: plant, augmented plant and complete open-loop transfer function with the controller. The resulting decoupling is illustrated in Figure 4.22.

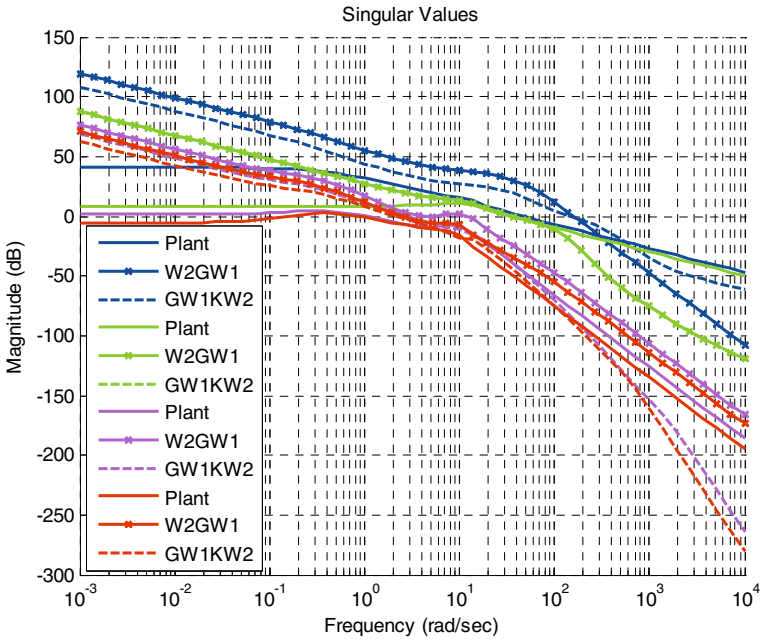

Fig. 4.21 Singular values resulting for loop-shaping design.

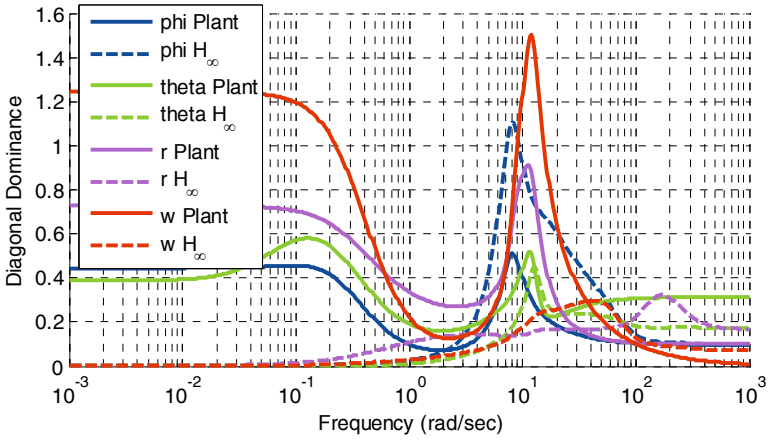

Fig. 4.22. Inner-loop decoupling using H_∞ control with loop-shaping.

Gain at lower frequencies is higher than in the case of the PID controller, but higher than the one achieved in the LQG design. Hence, decoupling and bandwidth, agility, may be just between both previous designs. The behavior at high frequencies is acceptable but not as good as the one achieved with LQG design.

Agility Test: Velocity Tracking for a Specific Trajectory

The three controllers have been used to control the helicopter in a specific trajectory very similar to the one shown in Figure 4.23. The velocities tracked by all three controllers are shown in Figures 4.24 through 4.26. Clearly, the PID design, having the highest gain at lower frequencies, presents the lowest tracking errors. On the other hand, having the H_∞ design the most moderate low frequency gain, it presents relatively larger deviations.

Sensitivity

Figures 4.27 and 4.28 depict the maximum singular values of the sensitivity functions. In the case of the input sensitivity function, the PID controller displays the best behavior, while the LQG controller presents the highest sensitivity to input noise. The output complimentary sensitivity functions indicate that the PID controller presents the worst maximum value, since it presents high sensitivity to sensor noise.

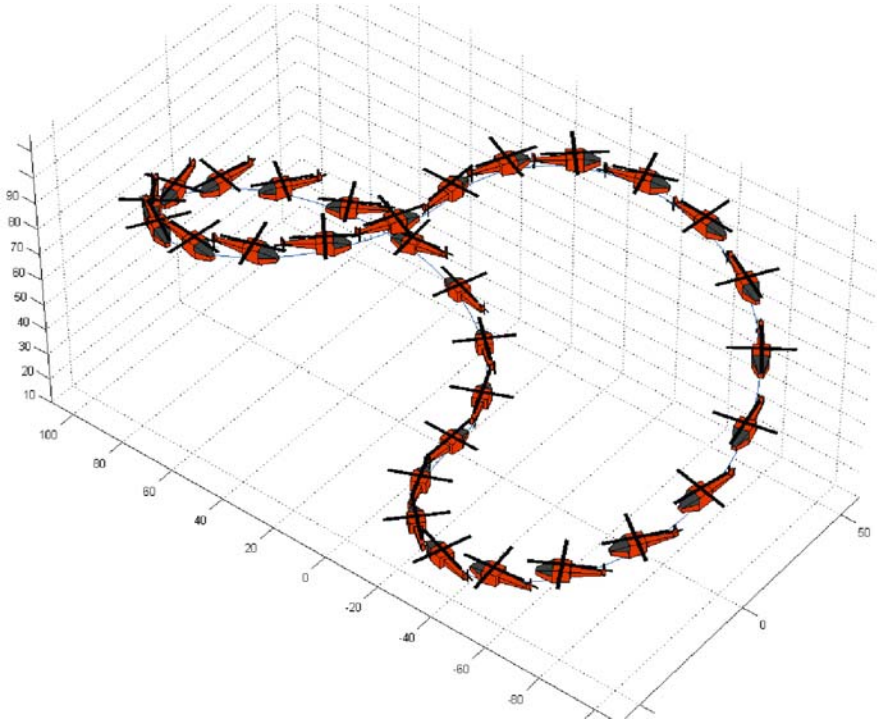

Fig. 4.23. Test trajectory.

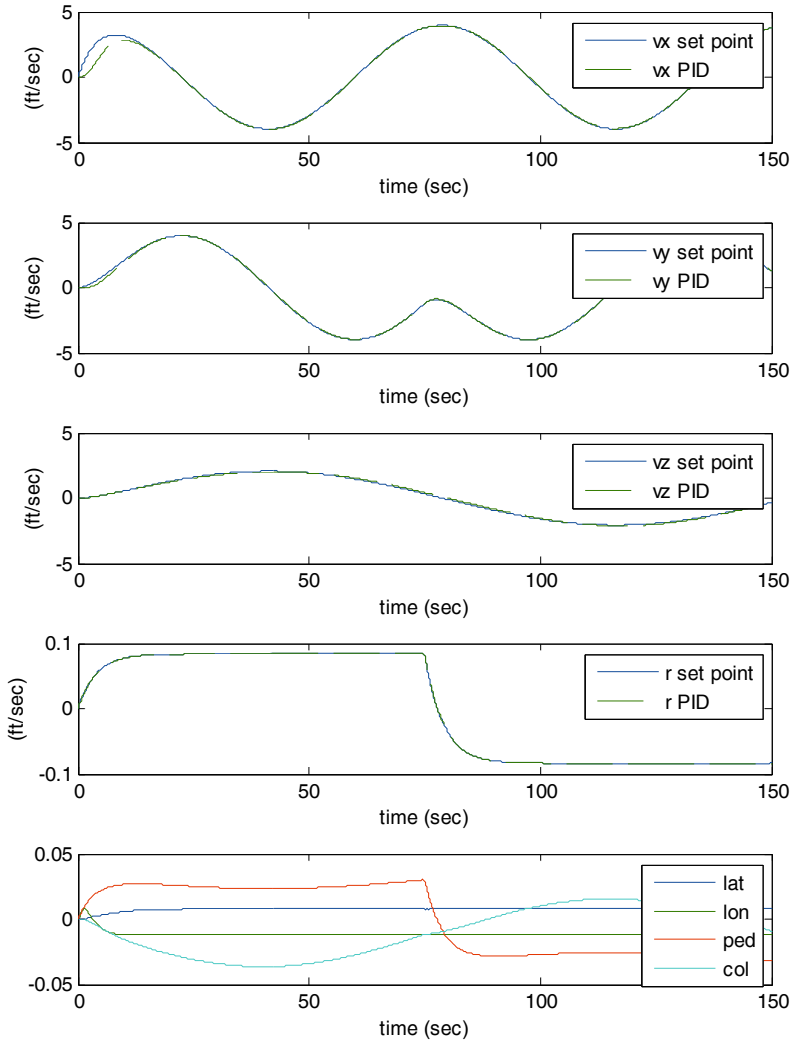

Fig. 4.24. Velocity tracking for PID controller.

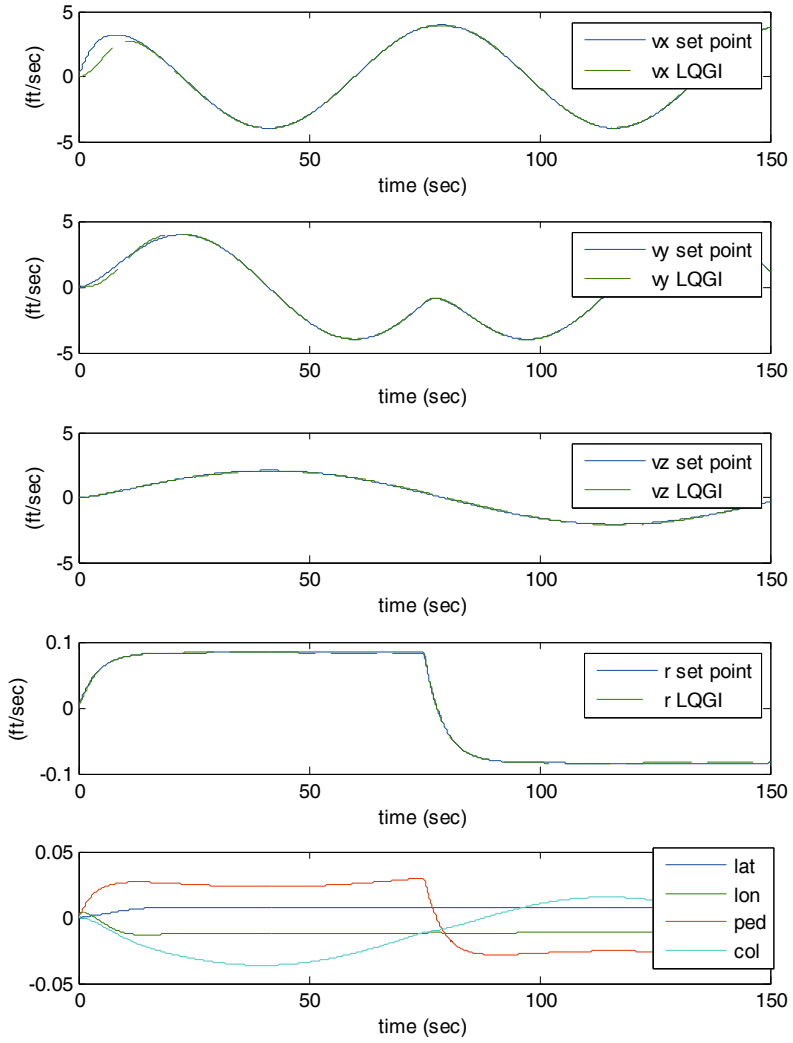

Fig. 4.25. Velocity tracking for LQGI controller.

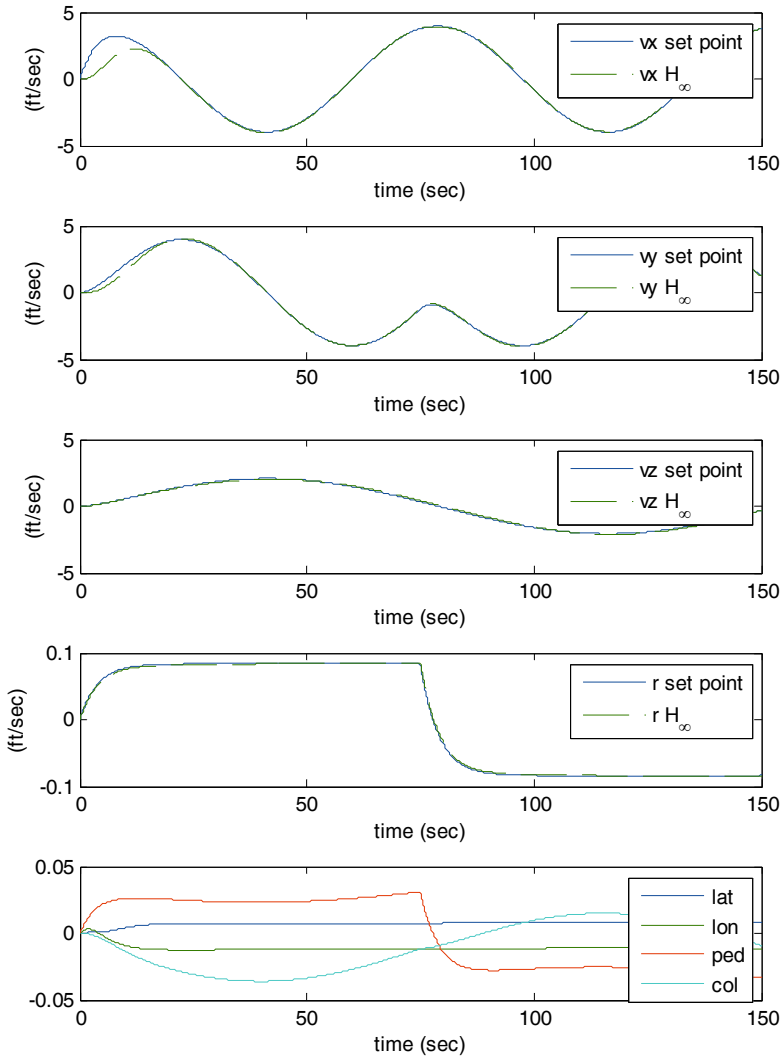

Fig. 4.26. Velocity tracking for H_∞ controller.

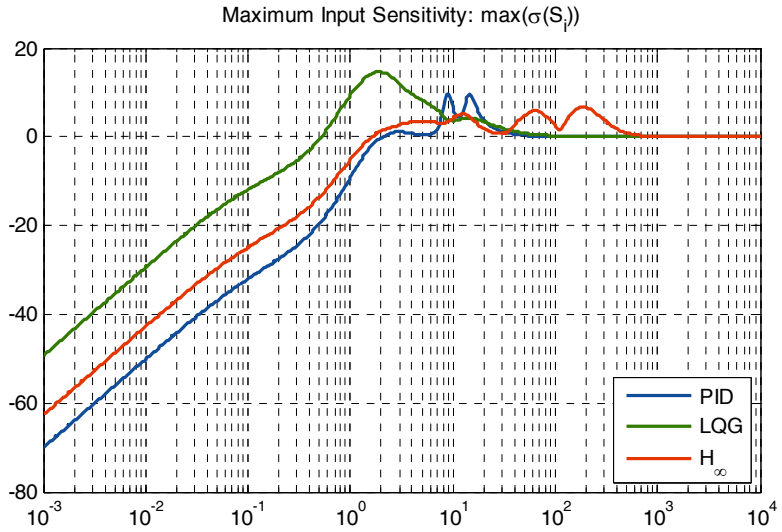

Fig. 4.27. Input sensitivity.

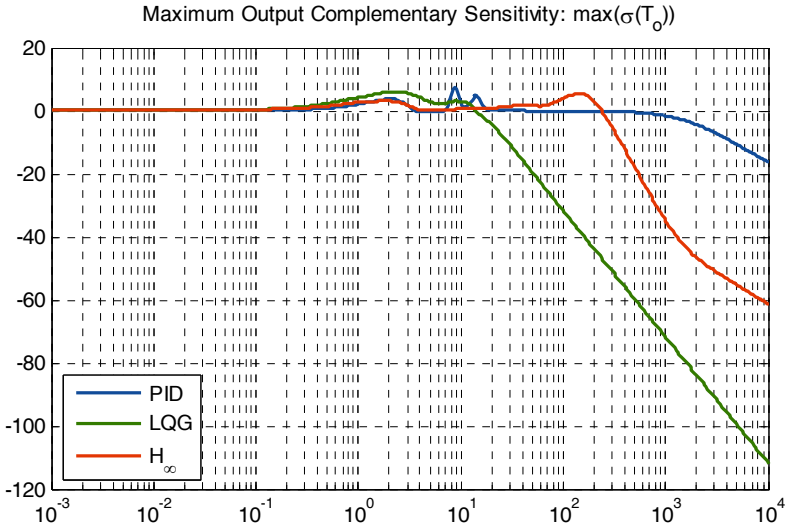

Fig. 4.28. Output complementary sensitivity.

Comparison of the Three Controllers

The three designs have been subject to three evaluation criteria that are extremely relevant for practical implementation of self-governing flights: agility, ability to handle noise and robustness.

A comparative study of the three designs reveals that designs are also subject to trade-offs and compromises. High degree of agility, low steady state errors, robustness against disturbances and robustness against parameter variations cannot be achieved at the same time. The three designs have strengths and weaknesses, and selection of a specific controller depends on the application.

The LQG design exposes a slightly more sluggish dynamic response than the other designs and the worst decoupling behavior of all three. However, it has excellent values for output sensitivity and robustness in general terms. The PID design focused on agility and decoupling; does not provide enough robustness and it is extremely sensitive to output noise. The H_∞ design, thanks to the additional design freedom provided by the loop shaping methodology, presents a good trade-off between agility, robustness and noise sensitivity.

4.6 Conclusions and Future Perspectives

This Chapter presented just a glimpse of controller design for small helicopters. Challenges imposed by unmanned helicopters have contributed positively to advancing theory and applications of control theory, data fusion, flight control systems, and computer vision. New research fields have emerged or gained new relevance as is the case of the SEC program that has helped identifying shortcomings and challenges in computer-based implementation of control systems.

Stronger demands for higher autonomy levels will lead to improving collection and fusion of sensory data and perception provided by diverse suites of sensors, computer vision algorithms and better hardware. Likewise, higher reliability requirements will lead to development of highly intelligent fault-tolerant control systems supporting higher autonomy levels.

However, there are still limitations that prevent deployment of autonomous helicopters in envisioned applications. These limitations not only stem from the constrained payload capabilities and flight endurance of small size helicopters, but also from perspectives of control, autonomy, human robot interaction, and reliability. Most successful autonomous

flight control experiments have been carried out under controlled conditions and usually under the supervision of ground operators.

Most nonlinear or hybrid control techniques found in the literature are restricted to moderately successful simulation results. System identification procedures still require lengthy data collection experiments performed with the help of a skilled pilot. The vision of having UAVs deployed by non skilled personnel is yet to be reached. Similarly, the number of human operators per UAV is still represented by a ratio much greater than one.

Stated limitations have not stopped advancement of the unmanned systems field towards new goals as recommended by [43]. Goals in the next years incorporate coordination and cooperation in scenarios where multiple UAVs are required to be deployed. This has generated a profusion of research work in topics such as formation control, pursuit evasion games, swarming, flocking, etc. It is expected that in the near future, all these new theories will blend with intelligent fault-tolerant low-level control systems giving rise to fully autonomous swarms of miniature helicopters.

References

1. Adams R. J. and Banda S. S., "Robust Flight Control Design Using Dynamic Inversion and Structured Singular Value Synthesis", *IEEE Transactions on Control Systems Technology*, 1(2):80–92, 1993.
2. Aerial Robotics Group, Department of Aeronautics and Astronautics, Massachusetts Institute of Technology, "The Development of a Small Autonomous Helicopter Robot for Search and Rescue in Hostile Environments", *Proceedings of the AUVSI Annual Symposium*, Baltimore, MD, July 12, 1999.
3. Amidi O., Kanade T., and Miller J. R., "Vision-Based Autonomous Helicopter Research at Carnegie Mellon Robotics Institute 1991-1997", *American Helicopter Society International Conference,* Paper T7-3, Japan, April 1998.
4. Avila-Vilchis J. C., Brogliato B., Dzul A. and Lozano R., "Nonlinear Modeling and Control of Helicopters", *Automatica*, 39:1583–1596, 2003.
5. Balas G., Chiang R., Packard A. and Safonov M., *Robust Control Toolbox For Use with MATLAB*, The Mathworks, Inc., Natick, MA, September 2006.
6. Bendotti P. and Morris J. C., "Robust Hover Control for a Model Helicopter", *Proceedings, American Control Conference*, pages 682–687, Seattle, Washington, 1995.
7. Brooks R., "A Robust Layered Control System for a Mobile Robot", *IEEE Journal of Robotics and Automation*, 2(1):14–23, March 1986.
8. Brown R. G. and Hwang P. Y. C., *Introduction to Random Signals and Applied Kalman Filtering with MATLAB Exercises and Solutions*, John Wiley & Sons, 3rd Edition, February 2001.

9. Buskey G., Roberts J., Corke P., Ridley P. and Wyeth G., "Sensing and Control for a Small-size Helicopter", *Experimental Robotics*, B. Siciliano and P. Dario, Editors, VIII: 476–487, 2003.
10. Castillo C. L., Alvis W., Castillo-Effen M., Moreno W., and Valavanis K., "Small Scale Helicopter Analysis and Controller Design for Non-aggressive Flights", *Proceedings, IEEE International Conference on Systems, Man and Cybernetics*, Volume 4, pages 3305– 3312, October 2005.
11. Fagg A. H., Lewis M. A., Montgomery J. F. and Bekey G. A., "The USC Autonomous Flying Vehicle: An Experiment in Real-Time Behavior-Based Control", *Proceedings, IEEE/RSJ International Conference on Intelligent Robots and Systems*, pages 1173–1180, Yokohama, Japan, July 1993.
12. Frazzoli E., Dahleh M. A., and Feron E., "Trajectory Tracking Control Design for Autonomous Helicopters Using a Back Stepping Algorithm", *Proceedings, American Control Conference*, pages 4102–4107, Chicago, Illinois, June 2000.
13. Gavrilets V., Martinos I., Mettler B. and Feron E., "Control Logic for Automated Aerobatic Flight of a Miniature Helicopter", *Proceedings, AIAA Guidance, Navigation, and Control Conference and Exhibit*, California, August 2002.
14. Gavrilets V., Mettler B., and Feron E. *Dynamic Model for a Miniature Aerobatic Helicopter*, Technical report, MIT-LIDS report LIDS-P-2580, 2003.
15. Gavrilets V., Shterenberg A., Dahleh M. A. and Feron E., "Avionics System for a Small Unmanned Helicopter Performing Aggressive Maneuvers", *Proceedings, 19th Digital Avionics Systems Conference*, Vol. 1, 2000.
16. Goodwin G. C., Graebe S. F. and Salgado M. E, *Control System Design*, Prentice Hall, September 2000.
17. Huang H.-M., Pavek K., Albus J. and Messina E., "*Autonomy Levels for Unmanned Systems (ALFUS) Framework: An Update*", Proceedings, SPIE Defense and Security Symposium, March 2005.
18. International Aerial Robotics Competition – "*The Ultimate Collegiate Challenge*", http://avdil.gtri.gatech.edu/AUVS/IARCLaunch-Point.html.
19. Isidori A., Marconi L. and Serrani A., *Robust Autonomous Guidance, An Internal Model Approach*, Springer, 2003.
20. Johnson E. N., Debitetto P. A., Trott C. A. and Bosse M. C., "The 1996 MIT/Boston University/Draper Laboratory Autonomous Helicopter System", *Proceedings, 15th Digital Avionics Systems Conference*, pages 381–386, 1996.
21. Johnson E. N. and Kannan S. K., "Adaptive Flight Control for an Autonomous Unmanned Helicopter", *Proceedings, AIAA Guidance, Navigation, and Control Conference and Exhibit*, Monterey, California, August 2002.
22. Kahn A. D. and Foch R. J., "Attitude Command Attitude Hold and Stability Augmentation Systems for a Small-scale Helicopter UAV*", Proceedings, 22nd Digital Avionics Systems Conference*, Vol. 2, 2003.
23. Kim H. J. and Shim D. H., "A Flight Control System for Aerial Robots: Algorithms and Experiments", *Control Engineering Practice*, 11(12):1389–1400, 2003.

24. Kim S. K. and Tilbury D. M., "Mathematical Modeling and Experimental Identification of an Unmanned Helicopter Robot with Flybar Dynamics", *Journal of Robotic Systems*, 21:95–116, March 2004.
25. Koo J. T. and Sastry S., "Output Tracking Control Design of a Helicopter Model Based on Approximate Linearization", *Proceedings, 37th IEEE Conference on Decision & Control*, Tampa, Florida, USA, December 1998.
26. La Civita M., Papageorgiou G., Messner W.C. and Kanade T., "Design and Flight Testing of an H∞ Controller for a Robotic Helicopter", *Journal of Guidance, Control, and Dynamics*, 29(2):485–494, March– April 2006.
27. La Civita M., Papageorgiou G., Messner W. C., and Kanade T., "Integrated Modeling and Robust Control for Full-Envelope Flight of Robotic Helicopters", *Proceedings, IEEE International Conference on Robotics and Automation*, 2003.
28. La Civita M., Papageorgiou G., Messner W. C. and Kanade T., "Design and Flight Testing of a Gain-Scheduled H∞ Loop Shaping Controller for Wide-envelope Flight of a Robotic Helicopter", *Proceedings, American Control Conference*, Vol. 5, page 4195, 4200, June 2003.
29. Ljung L., *System Identification: Theory for the User*, 2nd Edition, Prentice Hall PTR, December 1998.
30. Ljung L., *System Identification Toolbox – For Use with MATLAB*, The Mathworks, Inc., Natick, MA, September 2006.
31. The Mathworks, Inc., Natick, MA, *Control System Toolbox – For Use with MATLAB*, September 2005.
32. Mcconley M. W., Piedmonte M. D., Appleby B. D., Frazzoli E., Feron E. and Dahleh M. A., "Hybrid Control for Aggressive Maneuvering of Autonomous Aerial Vehicles", *Proceedings, 19th Digital Avionics Systems Conference*, Vol.1, 2000.
33. McFarlane D. and Glover Ke. "*A Loop Shaping Design Procedure Using H∞ Synthesis*", IEEE Transactions on Automatic Control, 37:759–769, June, 1992.
34. Mejias L. O., Saripalli S., Cervera P. and Sukhatme G. S., "Visual Servoing of an Autonomous Helicopter in Urban Areas Using Feature Tracking", *Journal of Field Robotics*, 23(3):185–199, 2006.
35. Mettler B., Dever C. and Feron E., *Identification Modeling, Flying Qualities, and Dynamic Scaling of Miniature Rotorcraft*, NATO Systems Concepts & Integration Symposium, Berlin, May 2002.
36. Mettler B., *Identification Modeling and Characteristics of Miniature Rotorcraft*, Springer, 2002.
37. Mettler B., Tischler M. B. and Kanade T., "System Identification of Small-size Unmanned Helicopter Dynamics", *55th Forum of the American Helicopter Society,* Montreal, Quebec, Canada, May 25-27, 1999.
38. Micropilot Inc., http://www.micro-pilot.com, January 2007.
39. Montgomery J. F., Fagg A. H. and Bekey G. A., "The USC AFV-I: A behavior-based entry in the 1994 International Aerial Robotics Competition", *IEEE Expert, (see also IEEE Intelligent Systems and Their Applications)*, 10(2):16–22, 1995.

40. Morris J. C., Van Nieuwstadt M. and Bendotti P., "Identification and Control of a Model Helicopter in Hover", *Proceedings, American Control Conference*, pages 1238–1242, Baltimore, Maryland, June 1994.
41. Nguyen H. T. and Prasad N. R., *Fuzzy Modeling and Control*, CRC, March 1999.
42. Obinata G. and Anderson D.O., *Model Reduction for Control System Design*, Springer, 2001.
43. http://www.fas.org/-irp/program/collect/uav.htm, 2005.
44. Padfeld G. D., *Helicopter Flight Dynamics: The Theory and Application of Flying Qualities and Simulation Modeling*, Co-published by AIAA and Blackwell Science, 1996.
45. Prouty R. W., *Helicopter Performance, Stability, and Control*, Krieger Publishing Company, 2001.
46. Samad T. and Balas G., *Software-Enabled Control: Information Technology for Dynamical Systems*, Wiley-IEEE Press, February 2003.
47. Sanders C. P., DeBitetto P. A., Feron E., Vuong H. F. and Leveson N., "Hierarchical Control of Small Autonomous Helicopters", *Proceedings, 37th IEEE Conference on Decision & Control*, pages 3629–3634, Tampa, Florida, USA, December 1998.
48. Saripalli S., Naffin D. J. and Sukhatme G. S., "Autonomous Flying Vehicle Research at the University of Southern California", A. Schultz and L. E. Parker, Editors, *Multi-Robot Systems: From Swarms to Intelligent Automata*, Proceedings of the First International Workshop on Multi-Robot Systems, pages 73–82. Kluwer 2002.
49. Saripalli S., Roberts J. M., Corke P. I., Buskey G. and Sukhatme G. S., "A Tale of two Helicopters", *Proceedings, IEEE/RSJ International Conference on Intelligent Robots and Systems*, Las Vegas, Nevada, October 2003.
50. Saripalli S. and Sukhatme G. S., "Landing a Helicopter on a Moving Target", *Proceedings, International Conference on Robotics and Automation*, Rome, Italy, April 2007.
51. Shim D. H., Hoam C. and Sastry S., "Conflict-Free Navigation in Unknown Urban Environments", *IEEE Robotics & Automation Magazine*, 13(3):27–33, 2006.
52. Shim D. H., Kim H. J. and Sastry S., "Control System Design for Rotorcraft-Based Unmanned Aerial Vehicles Using Time-Domain System Identification", *Proceedings, IEEE International Conference on Control Applications*, Anchorage, Alaska, USA, September 25-27 2000.
53. Shim D. H., Kim H. J. and Sastry S., "Decentralized Nonlinear Model Predictive Control of Multiple Flying Robots in Dynamic Environments", *Proceedings, 42nd IEEE Conference on Decision and Control*, December 2003.
54. Shim D. H., Koo T. J., Hoffman F. and Sastry S., "A Comprehensive Study of Control Design for an Autonomous Helicopter", *Proceedings, 37th IEEE Conference on Decision & Control*, Tampa, Florida, USA, December 1998.
55. Shin J., Fujiwara D., Nonami K. and Hazawa K., "Model-Based Optimal Attitude and Positioning Control of Small-scale Unmanned Helicopter", *Robotica*, 23:51–63, 2005.

56. Shuzhi S. G. and Lewis F. L., Editors, *Autonomous Mobile Robots – Sensing, Control, Decision Making and Applications*, CRC Taylor & Francis Group, May 2006.
57. Skogestad S. and Postlethwaite I**.,** *Multivariable Feedback Control: Analysis and Design*, John Wiley &Sons, July 1996.
58. Sprague K., Gavrilets V., Dugail D., Mettler B., Feron E. and Martinos I., "Design and Applications of an Avionics System for a Miniature Acrobatic Helicopter", *Proceedings, 20th Digital Avionics Systems Conference*, Vol. 1, 2001.
59. Stein G., "Respect the Unstable", *IEEE Control Systems Magazine*, 23(4):12–25, 2003.
60. Stevens B. L. and Lewis F. L., *Aircraft Control and Simulation*, Wiley-Interscience, 2003.
61. Tischler M. and Cauffman M., "Frequency-Response Method for Rotorcraft System Identification: Flight Applications to BO-105 Coupled Fuselage/Rotor Dynamics"*, Journal of the American Helicopter Society*, 37:3–17, 1992.
62. http://www.rotomotion.com/prd UAV CTLR.html, January 2007.
63. *UAVs: Payloads and Missions*, Workshop held at the International Conference on Robotics and Automation, May 2006. Retrieved from: http://www.mem.drexel.edu/aerialRobotics/uavWorkshop2006.
64. Weilenmann M. F., Christen U. and Geering H. P., "Robust Helicopter Position Control at Hover", *Proceedings, American Control Conference*, pages 2491–2495, Baltimore, Maryland, June 1994.
65. Zhang P., Gu J., Milios E. E. and Huynh P., "Navigation with IMU/GPS/Digital Compass with Unscented Kalman Filter", *Proceedings, IEEE International Conference on Mechatronics & Automation*, 2005.
66. Zhou K. and Doyle J. C., *Essentials of Robust Control*, Prentice Hall, 1997.
67. Zhou K., Doyle J. C. and Glover K., *Robust and Optimal Control*, Prentice Hall, 1995.